

# RAINFALL VARIABILITY IN EXTRATROPICAL CYCLONES

DEDUCED FROM HALF-MINUTE RATES

by

Michael Jeffrey Rosen

B.S., The City University of New York  
(The City College of New York)  
(1967)

SUBMITTED IN PARTIAL FULFILLMENT

OF THE REQUIREMENTS FOR THE

DEGREE OF MASTER OF SCIENCE

at the

MASSACHUSETTS INSTITUTE OF TECHNOLOGY

May, 1971

Signature of Author .....

Department of Meteorology, May 17, 1971

Certified by .....

Thesis Supervisor

Accepted by .....

Chairman, Departmental Committee on Graduate Students

Lindgren  
**WITHDRAWN**  
JUN 8 1971  
**MIT LIBRARIES**

## RAINFALL VARIABILITY IN EXTRATROPICAL CYCLONES

## DEDUCED FROM HALF-MINUTE RATES

Michael Jeffrey Rosen

Submitted to the Department of Meteorology on May 17, 1971 in partial fulfillment of the requirements for the degree of Master of Science.

## ABSTRACT

This study concerns itself with the variability of the small-scale precipitation patterns in extratropical cyclones and its relationship to the large-scale features of the storm. The temporal distribution of rainfall intensity at West Concord, Mass. as well as the amount of the observed precipitation which was convective in character is determined for 28 extratropical cyclonic storms. Half-minute rainfall rates obtained from high resolution tipping bucket gauges are utilized for this purpose. The hourly means and variances of the distributions are then scrutinized to determine whether they adequately describe the features of these distributions and the extent to which the precipitation was convective and they are found to satisfactorily do so. Correlations of the mean and variance are then performed to each other and also to the position of the station with respect to the surface warm front and to the stability as measured by a vertical difference of pseudo potential wet-bulb temperatures. Significant correlations were discovered to exist between the variance and the rainfall intensity, the stability and the distance from the warm front, more specifically, it is seen that convective activity increases with increasing instability and with proximity of the warm front. A reduction of variance of 71% was obtained when these large scale parameters were used to determine the variance of the distribution.

The results, when expressed in linear regression equations, provide a method for forecasting the small-scale features of the precipitation pattern from a knowledge of the large scale parameters of the storm.

Thesis Supervisor: Dr. Pauline M. Austin  
Title: Research Associate

### ACKNOWLEDGMENTS

I would like to thank Dr. Pauline M. Austin without whose suggestions and necessary encouragement this thesis could never have been completed.

I would like to especially thank Marie L. Gabbe who at great inconvenience agreed to do the typing.

Appreciation is also expressed to Steven A. Ricci for his excellent work in the drafting of the figures.

## TABLE OF CONTENTS

CHAPTER 1	INTRODUCTION	6
CHAPTER 2	METHODS OF ANALYSIS OF RAIN GAUGE DATA	
	A. Sources of Data	10
	B. Processing of Data	10
	C. Computation of the Mean and the Variance	11
	D. Determination of the Degree to which the Precipitation is Convective	12
	E. Selection of Storms	14
CHAPTER 3	SELECTION OF LARGE-SCALE PARAMETERS	
	A. Rainfall Intensity	15
	B. Position with Respect to Large-Scale Features of the Storm	17
	C. Stability	20
CHAPTER 4	ADEQUACY OF THE HOURLY MEAN AND VARIANCE FOR DESCRIBING SMALL-SCALE FEATURES OF PRECIPITATION	
	A. Distribution of Half-Minute Precipitation Rates	23
	B. Subsynoptic Scales of Precipitation	26
CHAPTER 5	RELATIONSHIPS BETWEEN THE VARIANCE AND SYNOPTIC SCALE PARAMETERS	
	A. Relation of $\sigma^2$ to the Rainfall Intensity	29
	B. Dependence of $\mu$ and $\sigma^2$ on Position with respect to the Storm	29
	C. Relationship of the Mean and Variance to the Stability	33
	D. Regression Equations	36
CHAPTER 6	CONCLUSION	40
	FIGURES	42
	REFERENCES	53

## LIST OF FIGURES

- Figure 1. Hourly profiles of precipitation intensity
- Figure 2. Generalized cyclone model (after Boucher)
- Figure 3. Rainfall rate exceeded by 50% of half-minute intervals
- Figure 4. Rainfall rate exceeded by 10% of half-minute intervals
- Figure 5. Percentage frequency of hours in which the rainfall rate in  $x$  number of half-minute intervals is less than  $\mu + \sigma$ .
- Figure 6. Same as Figure 5 but for  $\mu + 2\sigma$
- Figure 7. Relationship of hourly mean and variance to synoptic scale rainfall
- Figure 8. Same as Figure 7 for small cells
- Figure 9. Same as Figure 7 for small mesoscale areas plus cells
- Figure 10. Distribution of values of  $\mu$  and  $\sigma^2$
- Figure 11. Distribution of  $\sigma^2$  around typical cyclonic storm

## CHAPTER 1

### INTRODUCTION

The purpose of this study is to uncover meaningful relationships between the small-scale precipitation patterns of extratropical cyclonic storms and certain large-scale properties of these storms. As a result of recent investigations, meteorologists have come to recognize the importance of understanding the interaction of small and large-scale features in extratropical cyclones; knowledge of small-scale motions and precipitation patterns could possibly be of considerable value in forecasting cyclonic development and precipitation amounts and, conversely, a knowledge of relationships between small and large scale features of these storms could make possible the prediction of the former from the latter.

Until recently, it had generally been believed that, at least in temperate latitudes, the synoptic-scale processes dominated within cyclonic storms. In the last decade, however, evidence has accumulated to the effect that this may not quite be the case. Newell (1960) suggested that cumulus convection may play a significant role in the vertical transports of heat and momentum within extratropical storms and thereby account, at least in part, for effects which had been previously attributed solely to the cyclonic scale motions. Charney and Eliassen (1964) proposed that both cumulus and cyclonic scale motions play a role in hurricane development; the cumulus cell by supplying the latent heat energy for driving the depression, and the depression

by producing the low level convergence of moisture into the cumulus cell. Danard (1964) then proposed that the release of latent heat also plays an important role in the dynamics of extratropical cyclones and subsequently (1966) discovered that incorporating the effects of latent heat led to a more accurate prediction of cyclogenesis.

Sanders and Olson (1967) showed that including the effects of latent heat into a quantitative precipitation forecasting model accounted for most of the deficiency which had previously been observed in the forecast precipitation amounts. They pointed out that although the role of the small-scale convective activity may be to redistribute rather than to enhance the precipitation within the storm area, the cumulus must be adequately dealt with if the details of the precipitation pattern were to be satisfactorily predicted.

In 1968, Gambo, by incorporating the latent heat of condensation by cumulus convection into that produced by the large scale motions found this small-scale contribution, in particular, to be an important factor in the prediction of cyclogenesis. Furthermore, the results of an investigation by Tracton (1969) showed that cellular convection embedded within an intense extratropical cyclone accounted for at least 30% of the total precipitation produced and, therefore, of the latent heat released. He also found that the small-scale motions accounted for a significant portion of the vertical transport of mass and momentum. This evidence leads to the conclusion that the sub-synoptic scale motions are of considerable meteorological significance in cyclonic storms and the consideration of these motions enables

cyclone development and precipitation amounts to be forecast to a much greater degree of accuracy.

Owing to the prohibitively dense network of observational stations required to describe the small-scale motions, however, a direct analysis of the interaction of the small and large scale features of cyclonic storms is at present not feasible. The small-scale motions, however, are reflected to a certain extent in the distribution and intensity of the observed precipitation. In this investigation, therefore, a statistical analysis is performed of the rainfall regime in extratropical cyclonic storms and its variability in time and space in the hope that the correlations which exist between this variability and certain synoptic scale parameters, chosen on the basis of physical reasoning, might provide insight into the relationships between the large and small-scale features of these storms.

The study is based on rainfall records which have exceptionally fine resolution in time. An attempt is made to define a parameter which adequately describes the temporal distribution of the rainfall intensity and which provides information as to the extent to which the precipitation is cellular in character. The suitability of the variance and mean for the distribution parameters is then discussed. Finally, correlations between these parameters and certain large-scale parameters of the storm are investigated; the latter include the convective instability and the position of the station under consideration with respect to the large scale features of the storm.



Although the extent of subsynoptic-scale features in cyclonic storms has been observed thus far primarily by radar, the analysis of rain-gauge data has been undertaken because of the facility with which they can be utilized in a statistical study of this nature. It is hoped that this investigation will provide a fruitful approach to the study of at least some of the sub-synoptic air motions and contribute to the development of realistic models of the small-scale features in rainstorms.

## CHAPTER 2

## METHODS OF ANALYSIS OF RAIN-GAUGE DATA

A. Sources of Data

This investigation is based on 28 cyclonic storms chosen from the period 1962-1970. Detailed tipping-bucket rain gauge records provided the data concerning the rate of precipitation. The gauges from which the records were taken are located at the M.I.T. field station at West Concord, Mass. and record rainfall rates with a time resolution of a few seconds in moderate to heavy rain. In all, three different gauges were operative during the period of interest. Whenever possible, data were taken from the Bean gauge which incorporates an 80" collector. One tip on this gauge amounts to a depth of precipitation equivalent to .009 mm. If heavy rain caused this gauge to become saturated or if the data were otherwise unavailable, traces from the Marshall gauges, which employ 38" and 19" collectors, were utilized.

B. Processing of Data

The original rain gauge traces contained information on the rate of precipitation in the form of tips, one tip corresponding to a certain amount of rain having fallen. To facilitate subsequent analysis, these data were processed in the following manner. First, the number of tips that occurred during each half-minute interval was counted and then, with the aid of formulas provided by laboratory calibrations, the

resulting quantities were converted to rainfall rates expressed in  $\text{mm hr}^{-1}$ . The formulas which were utilized are:

Gauge

$$\begin{array}{ll} 80'' & R (\text{mm hr}^{-1}) = n^{1.05} \\ 38'' & R = 1.9 n^{1.04} \\ 19'' & R = 7.6 n^{1.04} \end{array}$$

where  $R$  is the rainfall rate in  $\text{mm hr}^{-1}$  and  $n$  is the number of tips per half-minute interval. Much of the rain gauge data from the years 1962 and 1963 had already been so processed; however, because much of the synoptic data required for the subsequent analysis were not readily available for these years, a number of storms from more recent years were processed and included in the study.

C. Computation of the Mean and the Variance

Any attempt to correlate the large and small-scale features of cyclonic storms to each other would become extremely awkward if it were necessary to consider the rainfall rate for each half-minute interval in order to describe the small-scale motions. It is therefore desirable to find some parameter or parameters which would more readily lend themselves to correlation while retaining as much detail of the small-scale precipitation pattern as possible. Since these parameters must reflect the variability of the intensity of precipitation, it would seem reasonable to consider the mean and the variance of the rainfall rate as likely candidates. These quantities were therefore calculated for each individual hour of data from the half-minute rainfall rates

described above; a separate mean and variance were calculated for each hour. These quantities will henceforth be referred to as  $\mu$  and  $\sigma^2$  respectively.

Initially it is not at all clear that a distribution consisting of 120 values could be adequately described by just two parameters, and indeed this need not necessarily be the case particularly since it is known a priori that the distribution is not Gaussian owing to the  $0 \text{ mm hr}^{-1}$  lower bound. It was necessary, therefore, to explore the suitability of these parameters. The results of these explorations are described in Chapter 4.

#### D. Determination of the Degree to which the Precipitation is Convective.

The existence of precipitation areas on a smaller scale than and within synoptic-scale precipitation areas has been frequently noted in studies of precipitation patterns by investigators such as Cochran (1961) and Nason (1965). In 1969, Houze undertook to investigate directly the characteristics of such precipitation areas. He defined four distinct scales of precipitation areas; synoptic, large mesoscale areas, small mesoscale areas, and small cells, and in all of the storms he investigated, each area present seemed to contain within it all of the smaller scales, superposed one upon the other. The cause of these mesoscale areas is not as yet clear, however, it does not seem unreasonable to assume, as proposed by Melvin (1968), that the precipitation falling outside the cells in the small meso-

scale areas may have originally been condensed in the cells and carried out of them in the divergent upper portions of the cells.

In order that the parameters used to describe the small-scale features of the precipitation, i.e.,  $\mu$  and  $\sigma^2$ , be of the maximum usefulness, it is desirable that they give some indication as to the extent to which the precipitation is convective in character. Information concerning this aspect of the precipitation was extracted from the original rain gauge traces as explained below. An investigation was then performed to determine any relationships which might exist between  $\mu$  and  $\sigma^2$  and the amounts of convective precipitation. Results are discussed in Chapter 4.

Basically, most rain-gauge traces exhibit patterns like those given in Fig. 1 which show representations of these traces for periods of moderate, low, and intense convective activity. The sections of light, steady rainfall similar to those labeled A in the figure represent synoptic-scale precipitation. Plateaus of increasingly enhanced precipitation similar to B and C represent large and small mesoscale areas respectively from which the shower peaks, D, rise. Although the distinctions between various levels are not always clear cut, they are usually sufficiently obvious so that one can distinguish among the various scales of precipitation quite well; the results of two observers examining the same trace are not likely to differ by more than a few per cent.

The adequacy of this method for determining the relative amounts of precipitation produced by these different scales was tested by

Tracton (1969) by comparing results obtained in this manner to those obtained by an analysis of radar echoes. The amount of convectively produced rainfall determined from the radar agreed to within a few per cent of that determined from the rain gauge. It is assumed here that this agreement holds for precipitation produced by the mesoscale areas as well.

#### E. Selection of Storms

The only criteria, other than the availability of data, used to decide which storms to consider for this investigation were that the storm be fairly well organized, that there be sufficient precipitation observed at West Concord to make this study meaningful, and that the precipitation be in the form of rain, since snowfall could not be measured by the rain gauge. As a result, 28 storms consisting of approximately 450 hours of data were chosen for subsequent analysis. Included are all of the periods in which there was significant precipitation. In some storms, however, precipitation was observed to be intermittent and prolonged stretches occurred during which there was little or no precipitation. These periods were ignored.

## CHAPTER 3

## SELECTION OF LARGE-SCALE PARAMETERS

A. Rainfall Intensity

It is recognized that values of  $\sigma^2$  are not directly obtainable until after the precipitation has occurred, and then only from gauges which have exceptional time resolution. Therefore, this parameter would not be useful in forecasting the small-scale features of the precipitation, no matter how accurately it describes them, unless it could be deduced from quantities which are conventionally available in real time or whose values could be reasonably forecast prior to the storm's occurrence. Assuming, then, that  $\sigma^2$ , along with  $\mu$ , is found to adequately describe the desired characteristics of the precipitation, (in the actual investigation the suitability of these parameters was ascertained before further investigations were conducted) the next step is to seek some useful relationships between these parameters and several quantities describing the large-scale features of the storm.

First, the values of  $\sigma^2$  computed for the 450 hours described in Chapter 2 were correlated to the values of  $\mu$  computed for those hours. Although these values of  $\mu$ , the mean hourly rainfall rate, are intended to be used in conjunction with the variance to describe the small-scale features of the storm and, in fact, were obtained from the rain gauge data only after the precipitation had terminated, methods exist which enable one to make a forecast of the rate of precipitation up to 48 hours in advance of the storm.

Assuming that material disseminated by the Weather Bureau is the only information at one's disposal, the best means of obtaining such a forecast would seem to be from the Primitive Equation Model output. Forty-eight hour quantitative precipitation forecasts based on saturation deficit are made from this model and are issued once every twelve hours. These forecasts are presented as the amount of rainfall expected at a given station during the initial twelve hour period and for each succeeding six hour interval up to 48 hours. The Primitive Equation forecasts are for the most part reasonably accurate with the greatest error usually occurring as a marked deficiency in forecast precipitation near the southern fringe of the observed precipitation area in cases where the average relative humidity is as low as 70%. Information concerning the verification of these forecasts is presented in a semi-annual NMC publication entitled Numerical Weather Prediction Activities.

Unfortunately, interpolation of the forecast precipitation amounts is necessary if hourly rates of precipitation is desired. This interpolation could easily introduce errors of a factor of two or three or more into  $\mu$  even if the PE forecast is accurate. In this regard, information concerning rainfall rates to a resolution of a few minutes are available at the Weather Bureau and go into the preparation of the forecast that is eventually issued. Therefore forecasts of much better than those involving interpolation could probably be made at the Weather Bureau. Errors of a factor of 2 or 3 may also arise because current forecasting methods would probably be unable to re-



produce the high frequency fluctuations sometimes observed in the hourly mean rainfall rate in situations which involve intense precipitation; however, if some relationship can be obtained between  $\mu$  and  $\sigma^2$ , any forecast of  $\mu$ , no matter how crude, will be helpful.

#### B. Position with Respect to Large-Scale Features of the Storm

In an analysis of cold season East Coast storms, Boucher (1959) derived a cyclone model based on the fact that characteristic types of vertical radar echoes can be related to specific regions of the cyclonic precipitating cloud system (Fig. 2). He defined four distinct types of radar echoes which are most commonly observed as follows. Type I consists of closely spaced but distinct shallow (on the order of 500 m) cells or elements emanating from essentially a single level and most frequently associated with stratocumulus or altocumulus clouds. Resulting precipitation rates at the ground rarely exceed  $0.02 \text{ in hr}^{-1}$  ( $0.5 \text{ mm hr}^{-1}$ ). Type II is closely spaced cells originating at diverse levels and with ragged tops protruding above the region of a generally continuous echo which extends to the ground. Precipitation growth appears to occur principally in concentrated regions of updraft embedded in the large-scale precipitating cloud mass. Precipitation rates range to about  $0.5 \text{ in hr}^{-1}$  ( $12.5 \text{ mm hr}^{-1}$ ). Type III consists of generally uniform echoes produced by widespread and rather uniform rising motion but with cells occasionally embedded in the otherwise smooth echo. Most of the precipitation is of low intensity although it can reach  $0.5 \text{ in hr}^{-1}$  in cells. Finally, Type IV is described as

irregular echoes with tops at different levels generally associated with individual convective cells of the cumulus congestus or cumulonimbus variety. Figure 2 outlines areas of most frequent occurrence of the three predominating echo types. It is seen that Type III occupies the eastern and northern sectors of the cyclonic system well in advance of the center of lowest pressure, while Type I occupies the rear of the cyclone. Type II, occupying the region of the center of the cyclone and southward, overlaps Types I and III. Investigation of individual storms suggested that the transition from Type III to the more convective Type II echo is typically found within 200 miles of the cyclone track. Furthermore, the change of type was found to be rather abrupt, occurring in a matter of minutes. This suggests a change in the atmosphere from a state of uniform updraft to one where the vertical motion in the upper portion of the precipitating atmosphere is of a cellular nature.

Judging from the above description, which is taken from Boucher's paper, it seems eminently reasonable that  $\sigma^2$  would depend in some way on the position of the station in question with respect to the large scale features of the storm. The fact that the stability profile, on which the amount of convective activity is to a large extent dependent, varies with position in the storm system would lead one to draw similar conclusions.

Since most of the significant precipitation generally occurs to the east and north of the center of lowest pressure, this would seem to be the region of greatest interest. Tracton (1969) noted that, at

a certain location, the relative amounts of precipitation produced by stratiform and convective lifting were dependent on the position of that station relative to the surface warm front. Browning and Harrold (1969) noted, in investigations conducted in England, a large region of relatively uniform moderate rain 150-350 km ahead of the surface warm front and bands containing small areas of heavy rain aligned parallel to the front, forming close to the front and advancing ahead of it. Finally, Kreitzberg (1970) discovered tongues of warm moist air projecting from the warm frontal layer giving a leafed structure to the front. Convection is located above the stable leaves where potential energy is being released.

These investigations suggest that the position of the station with respect to the surface warm front may be a particularly important factor influencing  $\sigma^2$ . Correlations were therefore performed between the values of  $\mu$  and  $\sigma^2$  respectively and the perpendicular distance of the station (West Concord) from the surface warm front. This latter parameter was chosen because of its probable relevance and also because it is an easily identifiable entity readily obtainable from synoptic charts and easily forecast. The values used in this investigation were obtained from U.S. Weather Bureau surface charts. Interpolation was found to be necessary since these synoptic charts were available once every three hours for recent storms and only once every twelve hours for the others.

### C. Stability

The degree to which the atmosphere is unstable is generally utilized as an indication of possible convective activity in situations involving thunderstorms. The parameter usually relied upon in such situations is a Showalter or else a Lifted Index which are based upon the difference in temperature between a parcel of air at 850 mb and the same parcel after it has been lifted adiabatically to 500 mb. The index is then a measure of the extent to which the parcel would be warmer or colder than its environment. In cyclonic storms, where large masses of air are generally forced to ascend, temperature changes are being experienced throughout the entire layer, not just in a few isolated parcels, and this parameter would probably not be as useful. However, since situations in which  $\sigma^2$  assumes relatively large values in these storms are usually those associated with convective activity, it would not seem unreasonable to expect relationship between  $\sigma^2$  and some measure of the stability. Although such a relationship is implicit in relationships between  $\sigma^2$  and both  $\mu$  and the distance from the surface warm front, a more explicit representation might be advantageous provided a suitable parameter is found to represent the instability.

When a layer of air is forced to ascend, it may change from a stable to an unstable state when it becomes saturated, especially if the layer is significantly drier near the top than at the bottom. A layer within which this is the case is said to be convectively unstable. A measure of convective instability is the difference between

the pseudo potential wet bulb temperature at the bottom of the layer and that at the top of the layer. A positive difference indicates convective instability; the greater the difference, the greater the instability. Although a positive correlation might be expected to exist between this difference in wet bulb temperatures and , it is not known in what way these might best be correlated. Therefore, three different layers were considered, 850-700 mb, 850-500 mb, and 700-500 mb. The difference in pseudo potential wet bulb temperature between the bottom and the top of each of these layers was computed for all storm situations for which data were available. Unfortunately, no upper air data exists for any station in the immediate vicinity of West Concord. It was therefore necessary to use data from Portland, Me., and Nantucket, Mass. Furthermore, the necessary data were available only once during each twelve hour period. Since relatively high-frequency temporal fluctuations were found in  $\mu$  and  $\sigma^2$ , any correlation between these parameters for a particular hour and a parameter whose value could be ascertained only once every twelve hours would not be meaningful. Therefore, averages of the hourly values of  $\mu$  and  $\sigma^2$ , respectively, were taken over the periods  $(T_0-6)-T_0$ ,  $(T_0-3)-T_0$ ,  $(T_0-3)-(T_0+3)$ ,  $T_0-(T_0+3)$ , and  $T_0-(T_0+6)$ , where  $T_0$  is the time of the upper air observation. Correlations were then performed between each of these averages and the values of the aforementioned stability parameter (henceforth referred to as S) at Nantucket and Portland respectively. Correlations were also performed between these averages and the Showalter Index, more out of curiosity than with the expectation of meaningful results.

A number of assumptions were involved in the decision to use  $S$  as the stability parameter. In order that  $S$  be an accurate indication of the actual convective instability of the layer under consideration before the lifting was initiated, the values of pseudo potential wet bulb temperature that were measured must be equal to those that existed before the lifting took place. Also, it is desirable that not too much mixing between the layer and its environment has taken place so that the layer under consideration retains some semblance of its original identity. Concerning these assumptions, the pseudo potential wet bulb temperature is conservative with respect to dry and saturated adiabatic temperature changes and quasi conservative with respect to evaporation from falling rain so that if none of the instability has yet been released, the value of  $S$  which is utilized should not be too different from the actual convective instability of the layer that existed before the lifting began. The assumption that a significant amount of mixing has not taken place seems reasonable away from the storm center itself. However, in a large number of cases, especially as one moves farther away from the surface warm front, a considerable amount of instability will probably have already been released. It might therefore be more accurate to consider  $S$  as merely a general indication of the stability of the layer at the time in question rather than as a measure of the convective instability of the layer prior to the lifting.

## CHAPTER 4

## ADEQUACY OF THE HOURLY MEAN AND VARIANCE FOR DESCRIBING SMALL-SCALE FEATURES OF PRECIPITATION

A. Distribution of Half-Minute Precipitation Rates

Figures 3-6 show the distribution of the half-minute rainfall rates during each hourly interval, given the mean and the variance for that interval. As previously noted, it is not at all clear, a priori, that a distribution consisting of 120 half-minute intervals could be adequately described by just two parameters,  $\mu$  and  $\sigma^2$ . However, analyses of approximately 450 hours of data showed that these two parameters do describe the distribution surprisingly well.

Figures 3 and 4 show the rainfall rates exceeded by 50% and 10% of the half-minute intervals in any given hour, given  $\mu$  and  $\sigma^2$ . Although there are cases in which the distribution does not conform to the picture given by these graphs, the large majority of the cases do conform and given the mean and the variance, one can determine the entire distribution to a reasonable degree of accuracy (See Table 1). In 97% of the cases studied, for a given  $\mu$  and  $\sigma^2$ , no actual value was more than two isopleths removed from its value on the graphs for  $\mu < 8$ . No value was more than 4 isopleths removed for  $\mu > 8$ .

Table 1

Degree to which Isopleths fit points on  
Figs. 3 and 4 for  $\mu < 8$  .

	Fig. 3	Fig. 4
0	183	165
1	147	156
2	56	63
>2	10	12

\* The left hand side of the table gives the number of isopleths an actual value was removed from the value given in the figure (if the value of the 50% isopleth for a distribution with  $\mu = 3$  ;  $\sigma^2 = 10$  were actually 2.5, it would be one isopleth removed from its value of between 1 and 2 given in the figure. The values inside the table are numbers of points.  $\mu < 8$  396 points  $\mu > 8$  60 points.)

It is seen from Fig. 3 that for any given value of  $\mu$  , the rainfall rate exceeded by 50% of the intervals decreases as  $\sigma^2$  increases. This is the case because an increase in  $\sigma^2$  implies a larger number of half-minute intervals in which the rainfall rate is appreciably greater than the mean, although this number is usually far less than half the total number of intervals. If the mean is to remain unchanged, there must be a corresponding decrease in the more moderate values and consequently a decrease in the median point; hence, positively sloped isopleths. Another way of looking at this is that in order to keep the median value unchanged, an increase in  $\sigma^2$  implies an increase in  $\mu$  . Of course, it is theoretically possible to increase  $\sigma^2$  by decreasing the value of the smaller numbers. In reality, however, the presence of  $0 \text{ mm hr}^{-1}$  as a lower



limit to the distribution makes this, for all practical purposes, extremely rare and it may be ignored.

Fig. 4 portrays the fact that in most cases observed ( $\sigma^2 < 100-150$ ) the 10% isopleth tends to be negatively sloped. More specifically, the isopleths first tend to decrease to a minimum, the larger the value of the isopleth the larger the value of corresponding to the minimum point, and then slowly increase; the value of the positive slope is so small, however, that it can be represented by a horizontal line on the scale of the diagram. The behavior of these isopleths can be explained by the fact that for a given  $\mu$ , an increase in  $\sigma^2$  in most cases implies an increase in more than the top 10% of the values of the distribution and therefore an increase in the rainfall rate dividing the top 10% of the distribution from the remainder. In cases of high  $\sigma^2$  and relatively low  $\mu$ , however,  $\sigma^2$  is increased by increasing only the top three or four values of the distribution resulting in positively sloped isopleths. This is largely due to the presence of the lower bound of  $0 \text{ mm hr}^{-1}$ . It would be impossible, for example, to increase the top 10% of a distribution having  $\mu = 1$  above  $10 \text{ mm hr}^{-1}$  without setting some of the other values to below zero. In practice, however, hours in which  $\mu = 1$  and  $\sigma^2$  is large usually have 90% of their values below  $3 \text{ mm hr}^{-1}$ . It is seen then from Figs. 3 and 4 that for  $\mu$  remaining constant, a negatively sloped  $n\%$  isopleth indicates that an increase in  $\sigma^2$  implies an increase in more than the top  $n\%$  of the values of the distribution; while if the isopleths are positively

sloped, an increase in  $\sigma^2$  implies an increase in less than the top n% of the values.

An alternate method of describing the distribution is given in Figs. 5 and 6 which give the number of half-minute intervals in which the rainfall rate is less than  $\mu + \sigma$  and  $\mu + 2\sigma$  for  $\sigma^2 \gg 1$  and  $\sigma^2 < 1^*$ , the division being arbitrary. What these graphs indicate is that in a large majority of the cases, one should expect approximately 85% and 95% of the values to be less than  $\mu + \sigma$  and  $\mu + 2\sigma$  respectively.

Although it would be desirable, it is difficult to extract any useful information concerning the top two or three values of the distribution from  $\mu$  and  $\sigma^2$  other than the fact that in most cases these values are greater than  $\mu + 2\sigma$  and that the contribution of any of these single values to  $\sigma^2$  is  $(x - \mu)^2 / 120$  so that any rainfall rate for which the value of this expression is greater than  $\sigma^2$  could not possibly have occurred within the hour in question.

## B. Subsynoptic Scales of Precipitation

Figures 7-9 relate the mean and the variance of the distribution to the extent to which the precipitation occurring within the hour is synoptic, large mesoscale, small mesoscale, or cellular in character. In general, rainfall rates for these scales were observed to be 0-3, 2-6, 4-9, and 8- mm hr<sup>-1</sup> respectively with the overlap because the

---

\*

$\sigma^2 \gg 1$  for 347 hours and  $\sigma^2 < 1$  for 109 hours.

ranges differ in different storms. The graph shows the number of half-minute intervals out of a possible 120 as well as the percentage of the rainfall which can be considered synoptic or convective.

Fig. 7 relates  $\mu$  and  $\sigma^2$  to the synoptic scale rainfall. During hours in which  $\sigma^2$  is small, the rainfall is fairly steady. Because the upper bound of the rainfall rate for synoptic scale precipitation varies with each situation ( $3 \text{ mm hr}^{-1}$  may be synoptic in one storm and mesoscale in another) one cannot draw general conclusions concerning hours during which the rainfall rate is mostly in this transition range; therefore the existence of the region T on the graph, hours with low variances and rainfall rates in the transition region.

It is seen in Fig. 7 that for small values of  $\mu$ , synoptic scale rain takes up the larger part of the hour although its contribution to the total rainfall decreases as  $\sigma^2$  increases. This is a reasonable result since given  $\mu = 1 \text{ mm hr}^{-1}$ , for example, the minimum number of half-minute intervals during which the precipitation could possibly exceed the synoptic scale range,  $\geq 3 \text{ mm hr}^{-1}$ , is only forty, so in cases in which  $\mu$  is small, this very smallness places a lower bound on the number of intervals of synoptic scale rain and an upper bound on all other scales.

Increasing  $\sigma^2$  while maintaining  $\mu$  constant implies an increase in the rainfall rate of the upper values of the distribution which necessitates a corresponding decrease in the more numerous smaller values so that as  $\sigma^2$  increases the number of intervals

during which the precipitation is synoptic also increases. By the same token, large values of rainfall rate for a few of the intervals necessitate negligible values for the remainder, provided  $\mu$  is relatively small, so that one would expect the percentage contribution of synoptic scale precipitation to decrease as  $\sigma^2$  increases.

Figures 8 and 9 relate  $\mu$  and  $\sigma^2$  to that part of the precipitation which could be construed to have been derived from convective sources; Fig. 8 concerns itself with cellular precipitation alone while Fig. 9 includes both small mesoscale and cellular. Following lines of reasoning similar to those followed for Figs. 3, 4, and 7, one can see that the features of these two figures are basically what one might expect; that is, for a given value of  $\mu$ , the number of intervals during which these types of precipitation occur first increase, then remain constant, then slowly decrease as  $\sigma^2$  increases, while the per cent contribution to the total precipitation generally increases with  $\sigma^2$ . The existence of region T on Fig. 9 is for reasons similar to those given for Fig. 7.

The sample used in this study consists of the 450 hours of data whose values of  $\mu$  and  $\sigma^2$  are graphically portrayed in Fig. 10. There is a definite preponderance of points in the region of low  $\mu$  and  $\sigma^2$  but the results of this chapter should remain valid through  $\sigma^2 = 50$ . Although there is a dearth of points above this value, there is no reason to assume that the reasoning above changes in any way so that the extrapolations given in the figures are probably not too inaccurate.

## CHAPTER 5

## RELATIONSHIPS BETWEEN THE VARIANCE AND SYNOPTIC SCALE PARAMETERS

A. Relation of  $\sigma^2$  to the Rainfall Intensity

A relatively large positive correlation is found to exist between the hourly mean and variance of the precipitation rate. The correlation coefficient is 0.69. Because of the size of the sample, the correlation coefficient is significant at the 1% level. This is equivalent to saying that the probability of the populations of  $\mu$  and  $\sigma^2$ , from which these samples are derived, being uncorrelated is less than 1%.

Both  $\mu$  and  $\sigma^2$  were found to exhibit high-frequency fluctuations in time which seemed to be to a large extent in phase with each other. These fluctuations were noted to be present especially in situations of generally heavy rainfall. Explicitly, many though not all, prolonged periods of moderate or intense precipitation were characterized by one or two hours in which the values of  $\mu$  and  $\sigma^2$  were well above the average for the period in general, alternating with an hour or two in which they were well below the average. This result may be of some value in attempts to determine the spatial distribution of precipitation areas in cyclonic storms.

B. Dependence of  $\mu$  and  $\sigma^2$  on Position with Respect to the Storm

The distribution of  $\sigma^2$  with respect to the large scale features of the storm is depicted in Fig. 11. The position of the surface warm front relative to the station seemed to play a dominant role in the

determination of the variance. The behavior of  $\sigma^2$  in the vicinity of the warm front (Region A on Fig. 11) is discussed in detail below. In the 28 storms considered, by far the greater portion of the precipitation was observed in this region. Owing to the small number of cases in which significant precipitation was observed, such detailed results could not be obtained concerning the other areas of the storm. What information could be obtained for these areas is presented, separated by dashed lines, on Fig. 11.

Table 2 gives the percentage of cases in which various values of  $\sigma^2$  were observed as related to the distance from the warm front, negative distance is measured behind the front.

Table 2

Per cent Frequency of  $\sigma^2$  with Distance from  
the Surface Warm Front.

Distance from Warm Front (km)	$\sigma^2 < 5$	$5 < \sigma^2 < 10$	$10 < \sigma^2 < 20$	$\sigma^2 > 20$
> 200	100	0	0	0
100-200	58	27	15	0
0-100	39	22	20	19
-100 - 0	29	20	23	28

The values given in Table 2 were obtained from a composite of 28 storms and although the percentages given there varied from storm to storm, the general tendency for  $\sigma^2$  to increase as the warm front approached was observed in all storms. Although large values of

were occasionally observed in other quadrants of the storm, the amounts of precipitation observed, except for showers in connection with the cold front, was light as noted previously, and this study need not further concern itself with these areas. A definitive warm front or warm occlusion was found to be present in 22 of the 28 storms from which these results are derived and the large scale features of these storms assumed a configuration similar to that in the figure (The orientation of the cold front is for the most part immaterial). In the other storms, no definite warm front was identifiable owing to the fact that their location at sea rendered surface synoptic analysis difficult. However, in all of these storms, there existed a trough or similar discontinuity which seemed to produce results similar to those produced by a warm front and these storms were therefore included in the analysis.

The results shown in Table 2 are consistent with the models described in Chapter 3 in that there is a definite enhancement of convective activity in the proximity of the warm front. No value of above 5 was observed at a distance greater than 200 km from the front and in only 15% of the observations between 100 km and 200 km from the front was  $\sigma^2$  larger than 10. However, within 100 km of the front, a sharp increase in convective activity is noted with approximately 40-50% of the observed values of  $\sigma^2$  exceeding 10 and 20-30% exceeding 20, depending on which side of the front is considered. Table 3 presents this convective activity more explicitly. The values given in this table are obtained from Table 2 and Figs. 8 and 9 on the

assumption that the following rainfall rates, which seemed reasonable on the basis of observations, occurred:  $\mu = 2 \text{ mm hr}^{-1}$  for  $\sigma^2 < 5$  ;  $\mu = 3 \text{ mm hr}^{-1}$  for  $5 \leq \sigma^2 < 10$  ;  $\mu = 5 \text{ mm hr}^{-1}$  for  $10 \leq \sigma^2 < 20$  ;  $\mu = 8 \text{ mm hr}^{-1}$  for  $\sigma^2 \geq 20$  .

Table 3

Per Cent Contribution to the Total Precipitation by Cells and Small Mesoscale Areas and by Cells alone as a Function of the Distance from the Surface Warm Front.

Distance from Surface Warm Front	% of Precipitation Computed to be Cellular	% of Precipitation Computed to be Small Mesoscale or Cellular
> 200 km	< 5	< 20
100-200 km	13	30
< 100 km	33	59

The mean hourly rainfall rate,  $\mu$  , also has a tendency to increase with the approach of the warm front as is evidenced by the correlations given below. Although the behavior of this parameter is not as clear cut as that of  $\sigma^2$  , no value of  $\mu$  greater than  $5 \text{ mm hr}^{-1}$  is observed at a distance greater than 200 km ahead of the front.

A correlation of the distance from the surface warm front to  $\sigma^2$  and  $\mu$  resulted, as expected, in appreciable negative linear correlation coefficients of -0.39 and -0.26 respectively. Indications were, however, that since  $\sigma^2$  remained relatively small for distances ranging from 600 km up to 200 km from the front and then rapidly increased with the approach and passage of the front, a correlation



of  $\sigma^2$  to some function of the reciprocal of this distance might prove more fruitful. Therefore a correlation of  $\sigma^2$  to a function

Z was performed where Z is defined as

$$Z = \frac{1}{100 + l}$$

and  $l$  is the distance from the warm front which becomes negative after the frontal passage. This is equivalent to correlating  $\sigma^2$  to the reciprocal of the distance from a surface parallel to and 100 km behind the warm front. The resulting correlation coefficient was calculated to be +0.49 while the correlation coefficient of Z to  $\sigma^2$  increased to only +0.29. Thus, the use of Z explained more of the variation of  $\sigma^2$  independent of  $\mu$  than merely the use of  $\mu$ . All of the correlation coefficients presented in this section are significant at the 1% level.

### C. Relationship of the Mean and Variance to the Stability

Table 4 gives the results of the correlations of  $\mu$  and  $\sigma^2$  to the stability parameter described in Chapter 3. Correlations to the Showalter Index are included for the purposes of comparison. Since the upper air data necessary to obtain these stability parameters were available only every twelve hours, only 63 pairs were used in each correlation. Therefore, only correlation coefficients with absolute values greater than 0.34 are significant at the 1% level. Considering first  $\sigma^2$  it is at once evident that those coefficients pertaining to Portland, Me. as well as those evaluated at Nantucket between 700 mb and 500 mb can be discarded and excluded from further consideration.

Those coefficients of any significance (those evaluated for Nantucket between 850-700 mb and between 850-500 mb and, surprisingly enough, the Showalter Index) show no distinct preference for any particular time period. Turning to  $\mu$ , one is hard put to find anything of any major significance. However, what indications there are seem to point to a preference for  $\mu$  evaluated for those time periods occurring during and shortly after the evaluation of the stability parameter.

These results are consistent with physical considerations in that the rate of precipitation occurring at a station represents instability which has already been released so that one would expect to find the greatest correlations to exist when the stability parameter is evaluated prior to and upstream from the rainfall rate. In most storms considered, the 850-500 mb level winds showed a strong southerly component so that Nantucket would indeed be upstream whereas Portland would not be. Also the fact that the layers of any significance are 850-700 mb and 850-500 mb, and that a significant correlation is found to exist with the Showalter Index which is evaluated between 850 and 500 mb, is consistent with the fact that the base of most intense convective activity is generally in the vicinity of the 850 mb level.

Since the correlations with  $\sigma^2$  showed no distinct time preference, those evaluated for periods slightly prior to  $T_0$  tend to show the maximum correlation of  $\sigma^2$  to the stability independent of  $\mu$ .

Table 4

Correlation Coefficients between  $\mu$  and  $\sigma^2$  and Stability

Time Interval	Correlations of Stability to $\sigma^2$							
	ACK 850- 700 mb	PWM 850- 700 mb	ACK 850- 500 mb	PWM 850- 500 mb	ACK 700- 500 mb	PWM 700- 500 mb	ACK Showalter Index	PWM
$(T_o-6)-T_o$	0.33	0.22	0.42	0.30	0.13	0.22	-0.36	-0.28
$(T_o-3)-T_o$	0.33	0.04	0.50	0.08	0.21	-0.17	-0.53	-0.08
$(T_o-3)-(T_o+3)$	0.40	0.19	0.31	0.05	-0.08	-0.29	-0.51	-0.14
$T_o-(T_o+3)$	0.35	0.23	0.36	0.22	0.08	0.19	-0.51	-0.24
$T_o-(T_o+6)$	0.29	0.01	0.47	0.20	0.22	0.38	-0.44	-0.12

Correlations of Stability to $\mu$								
$(T_o-6)-T_o$	0.06	-0.09	0.00	0.09	-0.06	0.04	0.00	-0.10
$(T_o-3)-T_o$	-0.15	-0.04	0.00	-0.22	0.15	-0.07	-0.13	0.13
$(T_o-3)-(T_o+3)$	0.25	-0.25	0.28	-0.26	0.03	-0.21	-0.39	0.21
$T_o-(T_o+3)$	0.22	-0.16	0.31	-0.13	0.10	0.16	-0.42	0.14
$T_o-(T_o+6)$	0.21	-0.16	0.31	0.02	0.15	0.26	-0.30	0.03

% of Variance of  $\sigma^2$  explained by  $\mu$  and Stability  
(47% explained by  $\mu$  alone)

$(T_o-6)-T_o$	0.55	0.56	<u>0.66</u>	0.53	0.51	0.52	0.61	0.52
$(T_o-3)-T_o$	<u>0.66</u>	0.48	<u>0.73</u>	0.51	0.48	0.49	<u>0.66</u>	0.50
$(T_o-3)-(T_o+3)$	0.53	0.60	0.48	0.53	0.48	0.52	0.54	0.56
$T_o-(T_o+3)$	0.52	0.59	0.51	0.58	0.48	0.48	0.53	0.59
$T_o-(T_o+6)$	0.50	0.49	0.55	0.51	0.49	0.52	0.54	0.50

#### D. Regression Equations

Having obtained significant correlations between  $\sigma^2$  and  $\mu$  and between  $\sigma^2$  and  $Z$  and, to a certain extent, between  $\sigma^2$  and the stability, it is possible to perform linear regressions on these parameters in order that these relationships be expressed in a more usable form. Using the resultant equations it would be theoretically possible, from forecasts of the synoptic parameters obtained by conventional methods, to obtain a crude forecast of  $\sigma^2$ . It should be mentioned at the outset, however, that these relationships are based upon a sample obtained from past storms and theoretically are valid only for those storms. Conclusions as to the validity of these relationships in future situations are only possible on the assumption that the sample used reliably represented these parameters in all extratropical cyclonic storms, past and future. It is not now known whether this is the case although the physical reasoning behind these relationships would lead one to believe that this sample is representative. Applications of these equations to future data would give some indication.

Considering first only  $\mu$  and  $\sigma^2$ , the relationship

$$(1) \quad \sigma^2 = 4.5 \mu - 7.6$$

obtains in which 47% of the variability of  $\sigma^2$  is explained. This line is plotted on Fig. 10 over the observed values of  $\mu$  and  $\sigma^2$ . It is seen from the figure that if, for some reason, an estimate only of  $\mu$  were available, even if this estimate were accurate, one would obtain at best only a general idea of what  $\sigma^2$  might be.

This situation is improved somewhat by the availability of an estimate of  $Z$ . In most instances, this should present little problem since forecasts of this parameter are usually readily obtainable from prognostic surface charts issued by the Weather Bureau. Taking into consideration both  $\mu$  and  $Z$ , the equation

$$(2) \quad \sigma^2 = 3.95 \mu + 567 Z - 8.9$$

results where the distance from the warm front is in km. This equation succeeds in explaining 57% of the variability of  $\sigma^2$ . An equation using the distance from the surface warm front,  $l$ , explicitly, explains only 53% of the variability of  $\sigma^2$  but is found to give a slightly better fit for  $l > 100$ -150 km.

$$(3) \quad \sigma^2 = 4.15 \mu - 0.02 l - 2.7$$

Both equations tend to give overly large values of  $\sigma^2$  if  $\mu$  and  $l$  are both large, however, in the sample this combination was found to occur only rarely.

If one now includes a stability parameter whose correlation to  $\sigma^2$  independent of  $\mu$  and  $Z$  (the correlation of  $S$  to  $Z$  was found to be about +0.6 for those stability parameters which correlated most highly with  $\sigma^2$  independent of  $\mu$ ) is the average of the highest correlations obtained, those underlined in Table 2, the equation

$$(4) \quad \sigma^2 = 4.6 \mu + 333 Z + 2.1 S - 9.0$$

results where  $S$  is a difference in pseudo-potential wet bulb temperature

between 850 and 700 mb in  $^{\circ}\text{K}$ . This equation explains 71% of the variability of  $\sigma^2$ . The figure at the right of this equation becomes -6.9 if the temperature difference is evaluated between 850 and 500 mb.

Since  $\mu$  and  $\sigma^2$  are of necessity expressed as three hour averages in their relationship to the stability, it becomes necessary to define the values of these parameters in this equation as three hour averages. The correlation coefficients involving the three hour averages used in the equation are:  $r_{\mu\sigma^2} = 0.68$ ;  $r_{\sigma^2 z} = 0.40$ ;

$r_{\mu z} = 0.18$ . The resulting values of  $\mu$  and  $\sigma^2$ , being three hour averages, must in some way be converted to their component hourly values if the use of Figs. 3-9 is desired to determine the various features of the distribution. The deviation from the average of the individual hourly values of  $\sigma^2$  is found to depend on the 3-hour average value to the extent that a correlation of +0.92 exists between them. If the following equation is used to determine  $\Delta\sigma^2$ ,

$$(5) \quad \Delta\sigma^2 = .585 \bar{\sigma^2} - 0.34$$

the values  $\bar{\sigma^2} - \Delta\sigma^2$ ,  $\bar{\sigma^2}$ , and  $\bar{\sigma^2} + \Delta\sigma^2$  provide reasonable estimates for the component hourly values of  $\sigma^2$ .

Similar considerations concerning  $\mu$  result in an analogous equation

$$(6) \quad \Delta\mu = .750 \bar{\mu} - 1.21$$

where the correlation coefficient between  $\Delta\mu$  and  $\bar{\mu}$  is +0.90.

The fact that equation (4) above involving  $\mu$  , Z , and S , explains only slightly more of the variability of  $\sigma^2$  than  $\mu$  and S alone (Table 2) leads to the conclusion that the contribution of Z to the explanation of  $\sigma^2$  is to a large part accounted for by the contributions of  $\mu$  and S. The correlation of +0.6 between Z and S indicates that the stability is dependent on the distance from the warm front.

Although the results involving S seem reasonable, the fact that only 63 values of S were used in the correlations along with the necessity of using equation 5 might make one uncomfortable. In this case, the use of equations 2 and 3 should lead to reasonably satisfactory results.

## CHAPTER 6

## CONCLUSION

The results of this investigation have shown that significant correlations exist between the distributions of rainfall intensity and convective activity in extratropical cyclonic storms and various large scale features of these storms; specifically the degree of convective activity is highly positively correlated to the stability and to the rainfall rate itself and negatively correlated to the distance from the surface warm front. Most of this activity appears to be concentrated within about 100 km of the front. It is possible that these small-scale features of the precipitation pattern are also influenced to an extent by geographical factors such as topography and position relative to a coastline; however, owing to the fact that this investigation concerned itself with only a single station, it was impossible to study these effects. There is no reason to believe, however, that the relationships derived here do not have a general validity beyond the one station actually studied.

This investigation also provides an empirical method which, assuming that the sample considered is representative of extratropical cyclonic storms in general, enables one to predict the degree of convective activity at a station and the probability of instantaneous rainfall rates from knowledge of the large scale features of the storm. This would entail utilizing the equations in Chapter 5 to determine  $\sigma^2$  from forecasts of the large scale



parameters and then employing the graphs presented in Chapter 4 to determine from  $\mu$  and  $\sigma^2$  the distribution of the rainfall rate with time and the amount of convective activity to be expected. The primary inaccuracies inherent in this method would appear to be the errors in the forecast large scale parameters as well as the fact that in even the best of the equations in Chapter 5, 29% of the variance of  $\sigma^2$  still remains unexplained. It would appear that compared to these, the errors involved in deriving the small-scale features from  $\mu$  and  $\sigma^2$  would be relatively small. This ability to predict the small-scale features of the precipitation pattern might serve to improve quantitative precipitation forecasting in general.

Future investigations should concern themselves with developing a more explicit representation of the spatial distribution of the convective activity, as well as the mesoscale areas, in extratropical cyclones. Also, attempts to more accurately determine the role of and incorporate the effects of convection in dynamical models of quantitative precipitation forecasting and cyclone development would be useful.

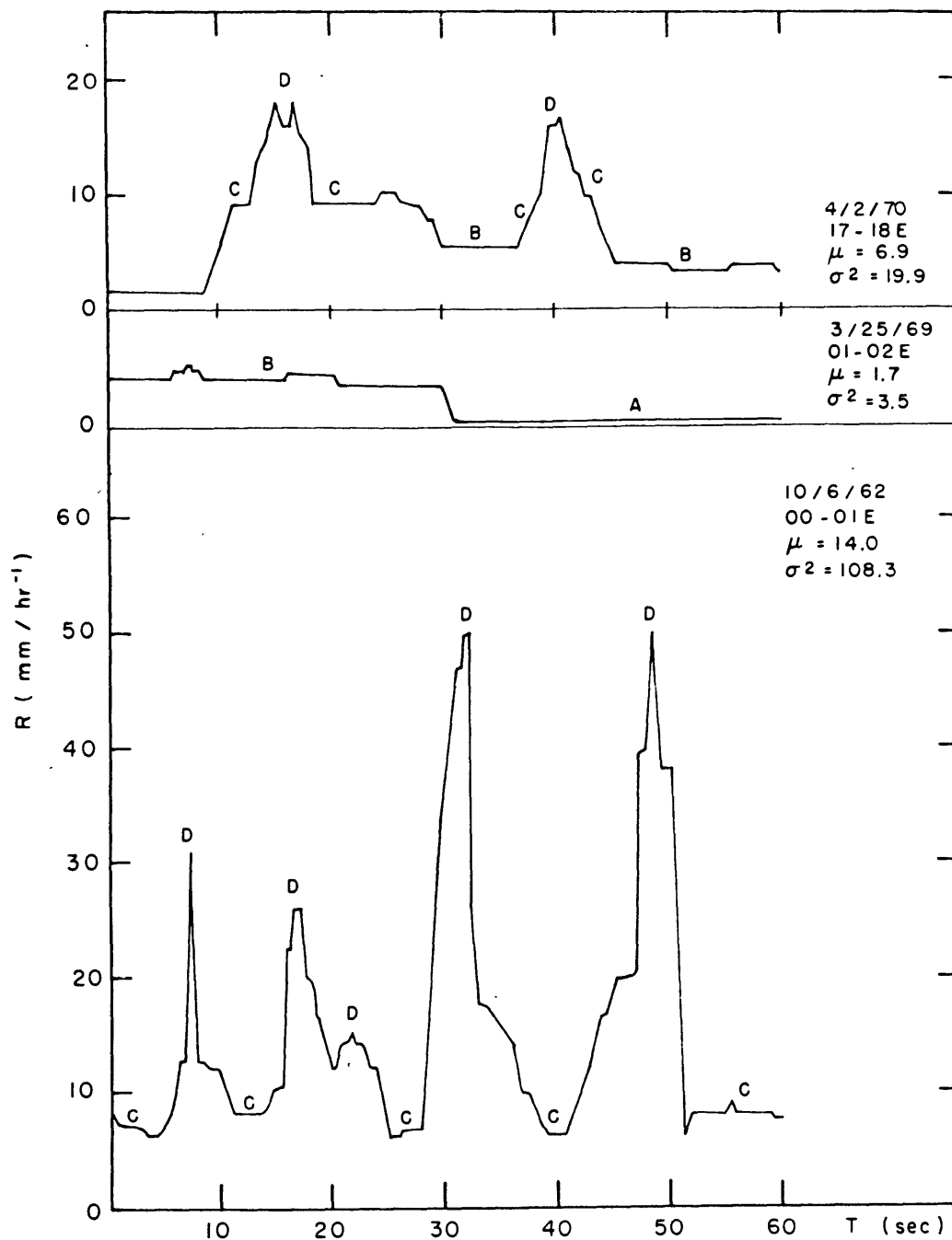


Figure 1. Hourly precipitation intensity for moderate, low, and intense convective activity

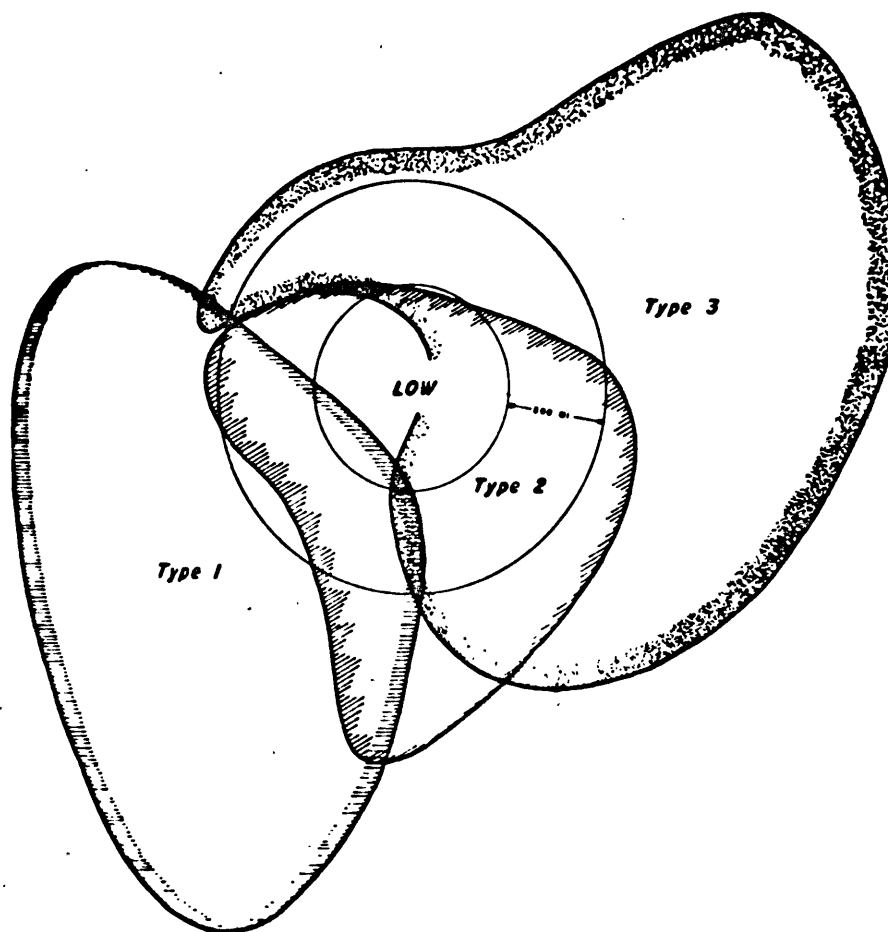


FIG. 3. Generalized cyclone model showing distribution of predominant types of vertical-beam radar echoes accompanying winter cyclones in New England. Circles are at radii of 200 and 400 mi.

Figure 2. Generalized cyclone model (after Boucher)

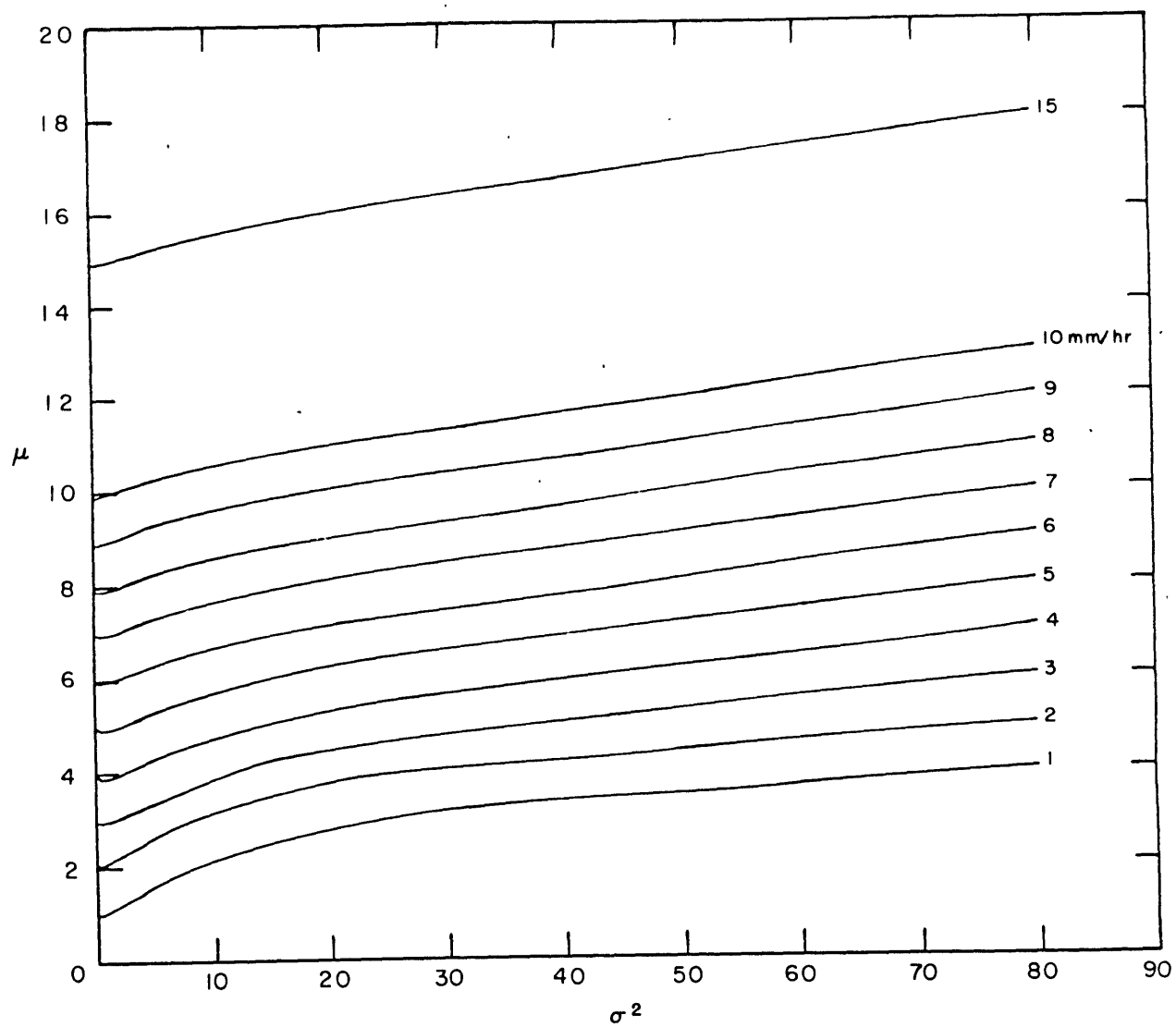


Figure 3. Rainfall rate in  $\text{mm hr}^{-1}$  exceeded by 50% of half-minute intervals as related to  $\mu$  and  $\sigma^2$

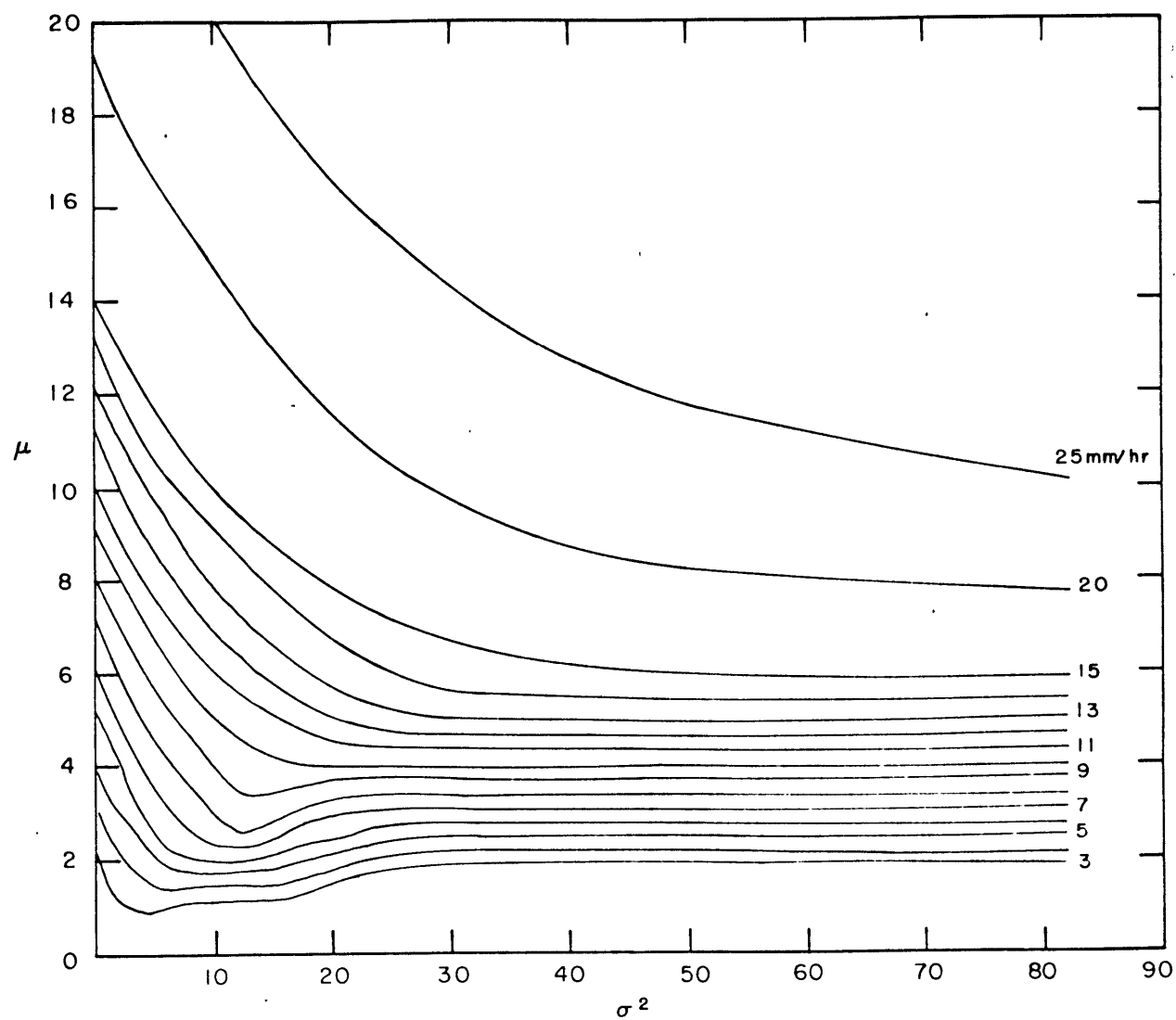


Figure 4. Rainfall rate in  $\text{mm hr}^{-1}$  exceeded by 10% of half-minute intervals

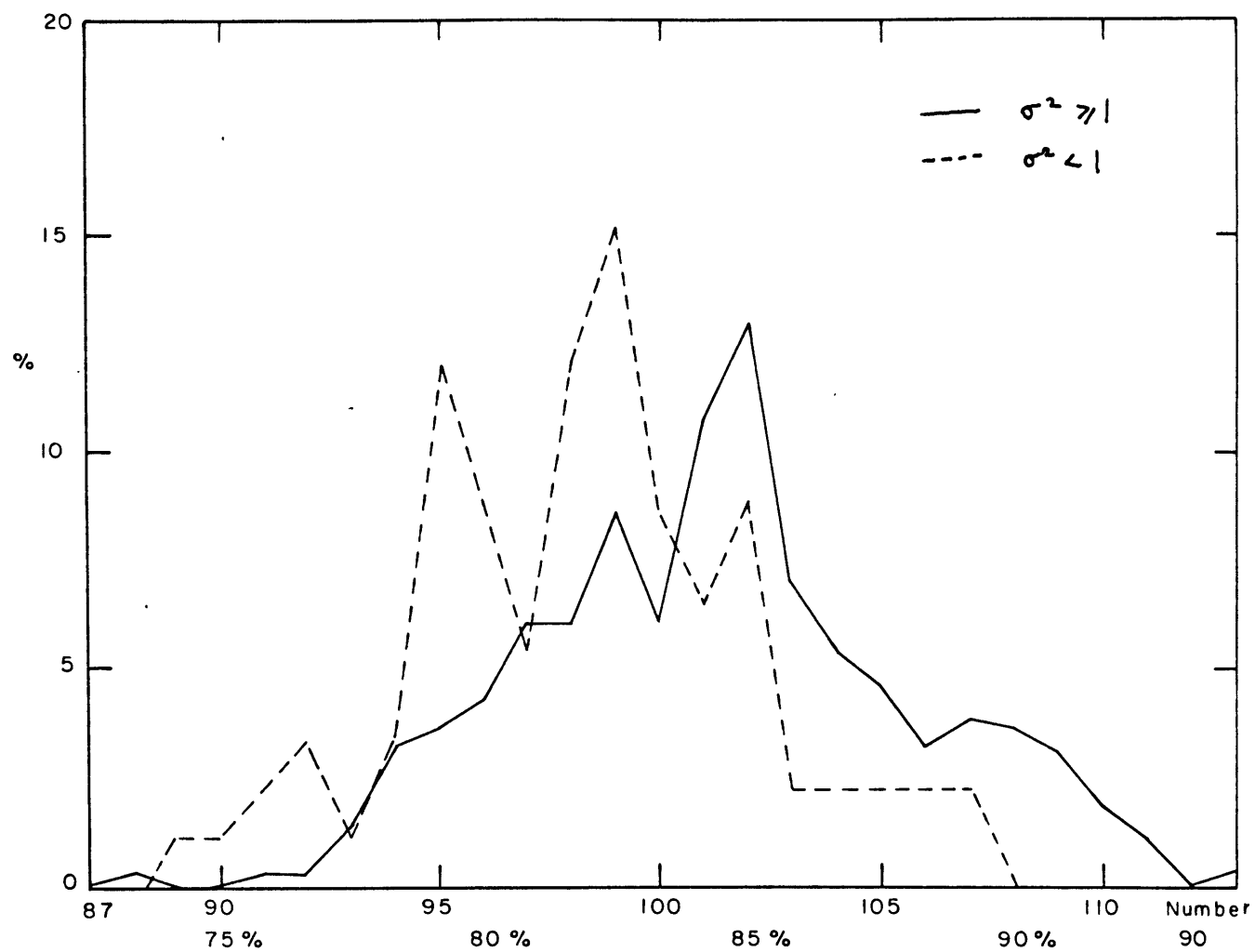


Figure 5. Percentage frequency of hours in which rainfall rate in x number of half-minute intervals is less than  $\mu + \sigma$ .

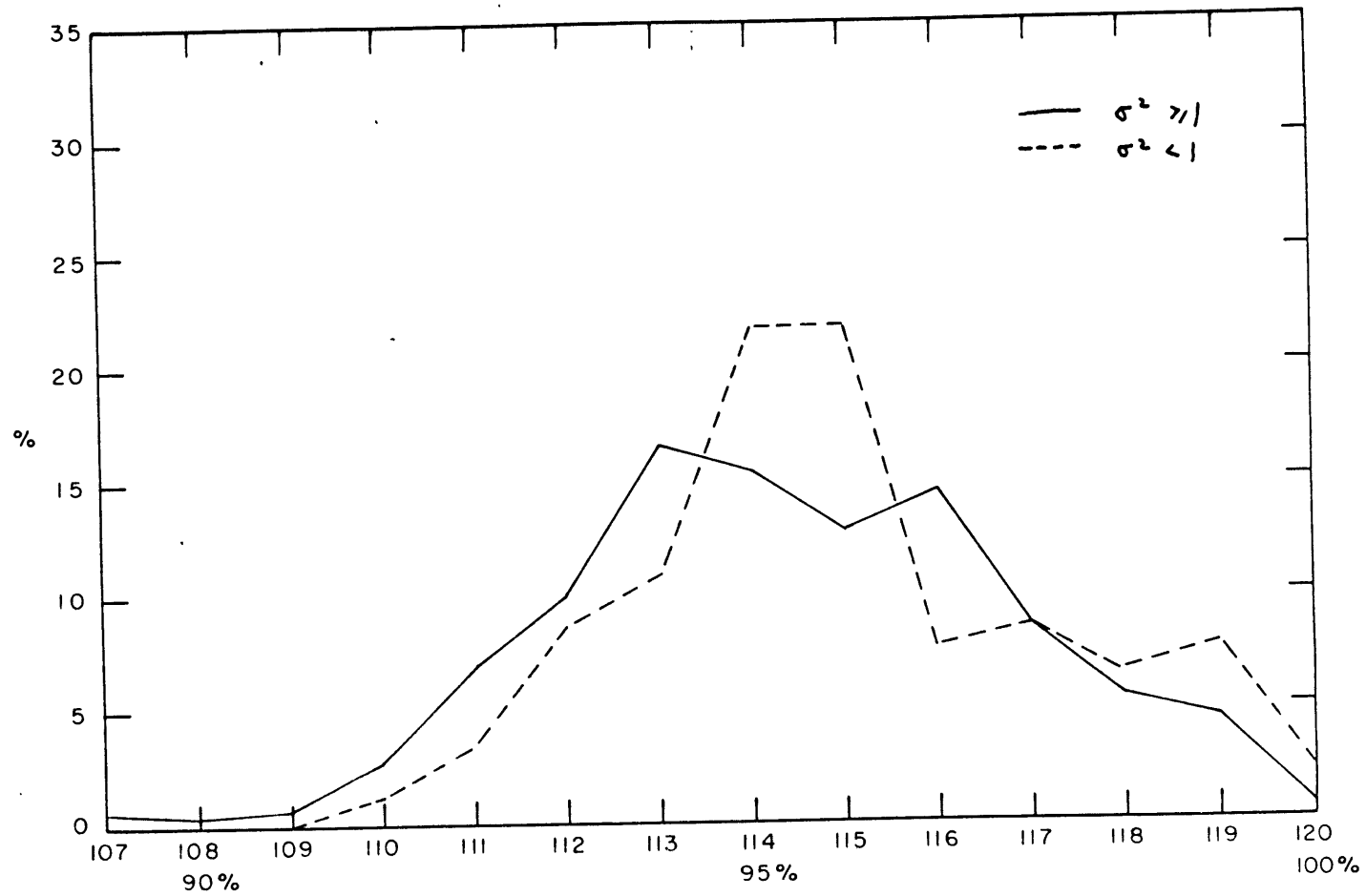


Figure 6. Same as Fig. 5 but for  $\mu + 2\sigma$ .

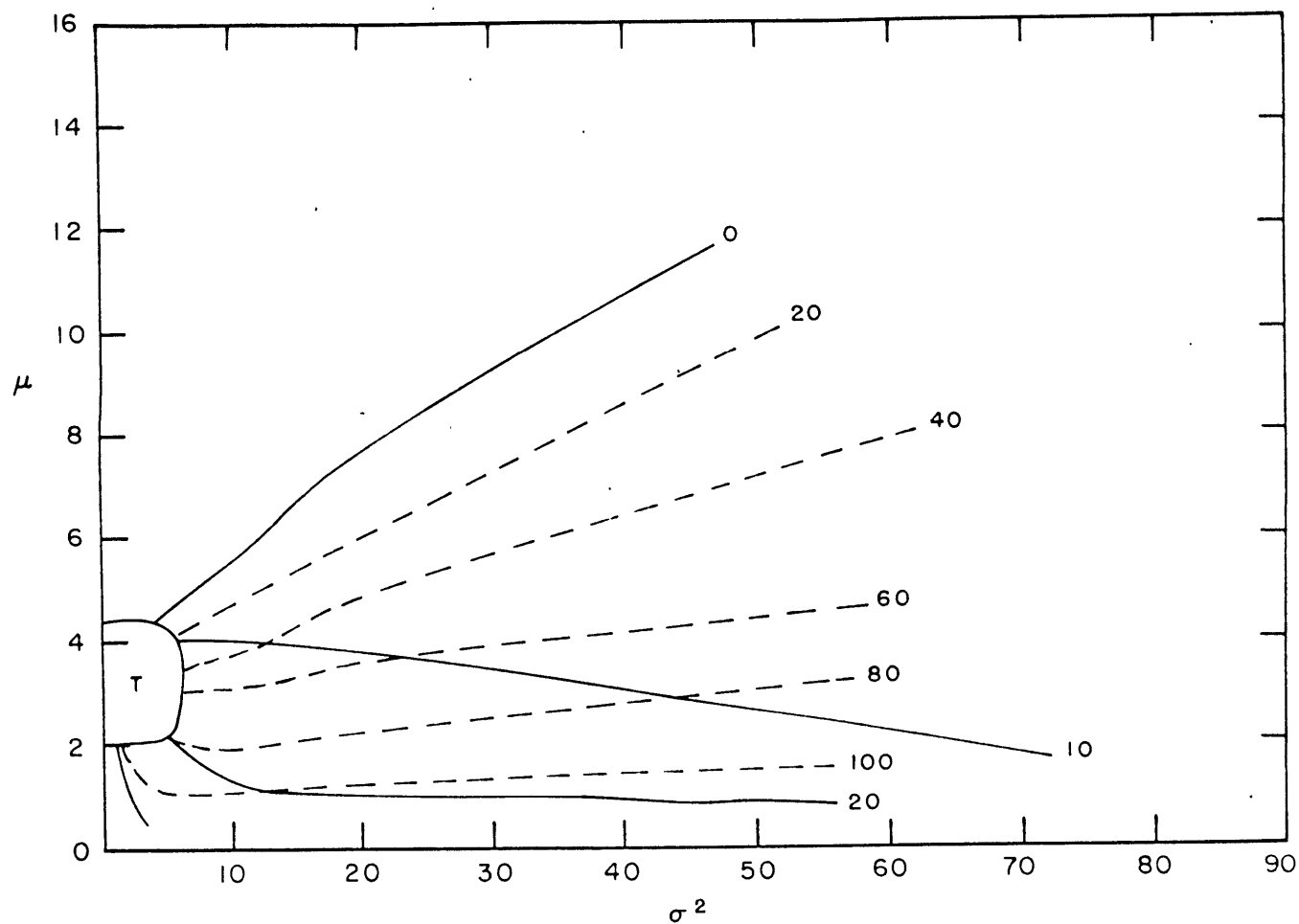


Figure 7. Relationship of hourly mean and variance to synoptic scale rainfall  
 ----- Number of half-minute intervals  
 \_\_\_\_\_ Percent of hourly rainfall which is synoptic in character



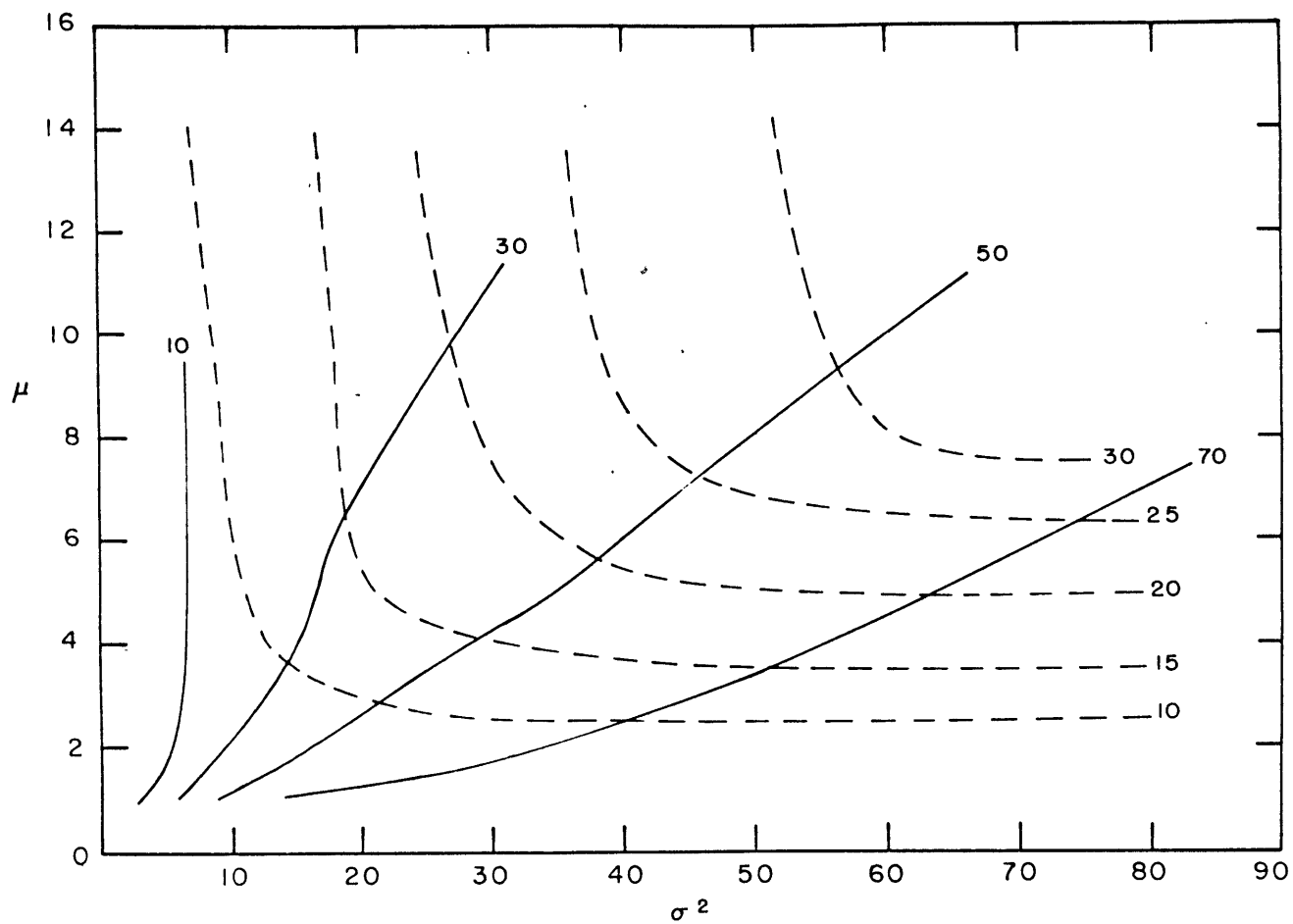


Figure 8. Same as Fig. 7 for small cells

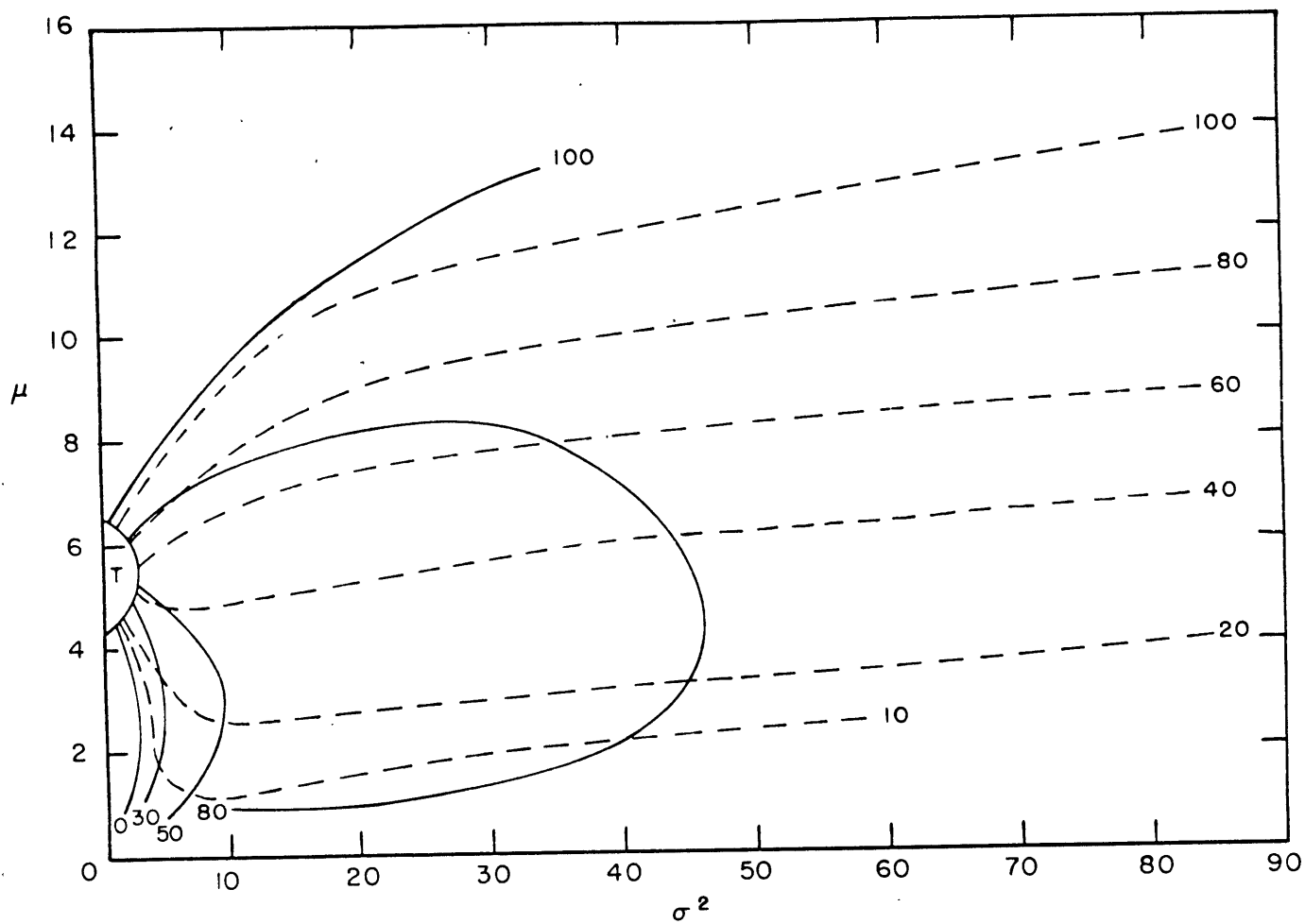


Figure 9. Same as Fig. 7 for small mesoscale areas plus cells

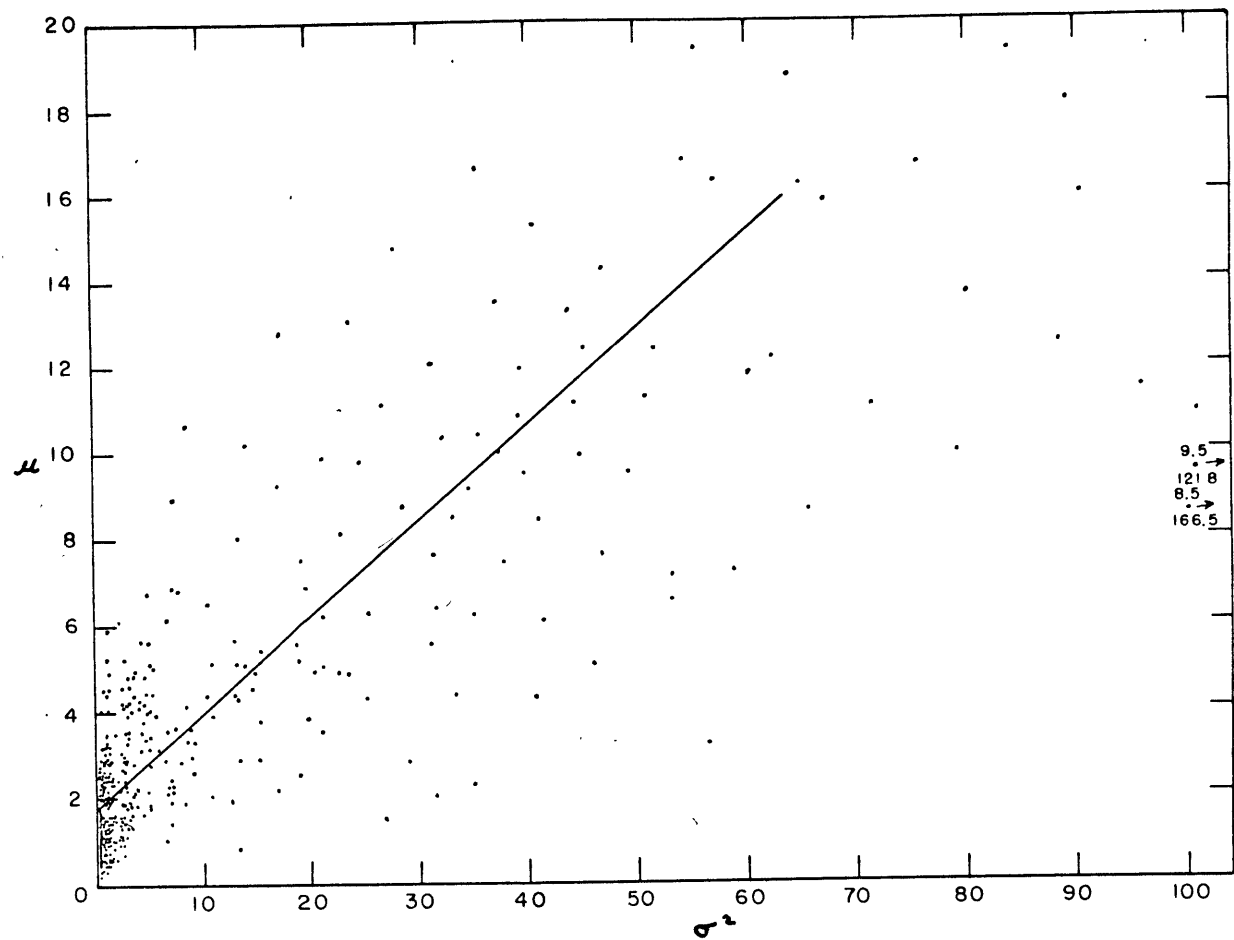


Figure 10. Distribution of values of  $\mu$  and  $\sigma^2$  used in this study

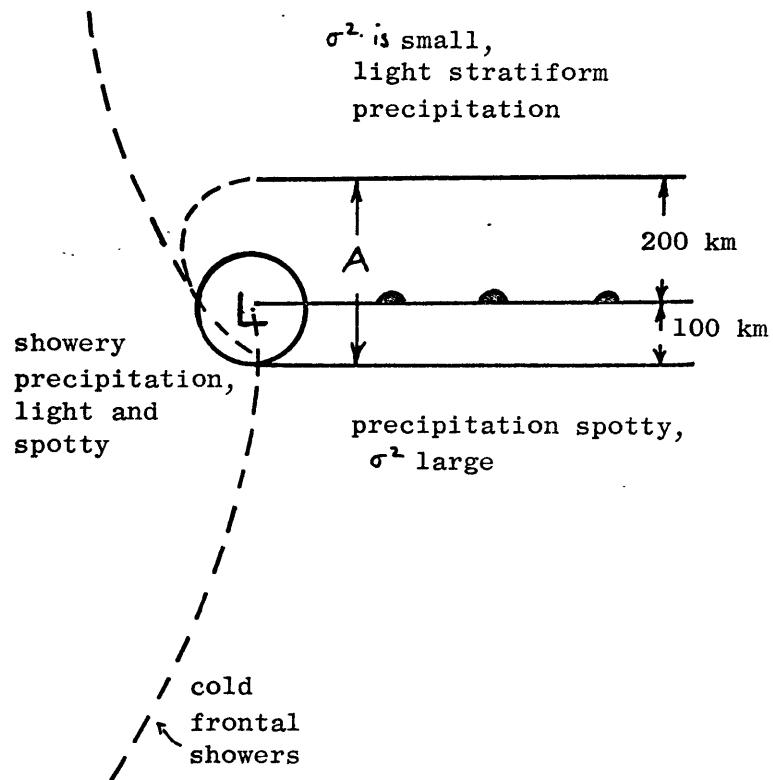


Figure 11. Distribution of  $\sigma^2$  around typical cyclonic storm

## REFERENCES

- Austin, P.M., 1968: Analysis of small-scale convection in New England. Proc. of the Thirteenth Radar Meteorological Conference, American Meteorological Society, Boston, Mass., 210-215.
- Boucher, R.J., 1959: Synoptic-physical implications of 1.25-cm vertical beam radar echoes. J. Meteor., 12, 312-326.
- Browning, K.A. and T.W. Harrold, 1969: Air motion and precipitation growth in a wave depression. Quart. J. R. Met. Soc., 95, 288-309.
- Charney, J.G. and A. Eliassen, 1964: On the growth of the hurricane depression. J.A.S., 21, 68-75.
- Cochran, H.B., 1961: A numerical description of New England squall lines. S.M. Thesis, Dept. of Met., MIT, Cambridge, Mass., 57 pp.
- Danard, M.B., 1964: On the influence of released latent heat on cyclone development. J. Appl. Met., 3, 27-37.
- Danard, M.B., 1966: On quasi-geostrophic numerical model incorporating effects of release of latent heat. J. Appl. Met., 5, 85-93.
- Elliott, R.D. and E.L. Hovind, 1964: On convection bands within Pacific coast storms and their relation to storm structure. J. Appl. Met., 3, 143-154.
- Gambo, K. 1968: Treatment of the interaction between the large-scale and convective motions in relation with the cloud amount and the stability factor. Proc. of the WMO/IUGG Symposium on Num. Wea. Pred. Tokyo, Japan, 1-10.
- Houze, R.A., 1969: Characteristics of mesoscale precipitation areas. S.M. Thesis, Dept. of Met., MIT, Cambridge, Mass., 77 pp.
- Houze, R.A., 1970: Proposal for Doctoral Research. Dept. of Met., MIT, Cambridge, Mass., 45 pp.
- Kreitzberg, C.W. and H.A. Brown, 1970: Mesoscale weather systems with an occlusion. J. Appl. Met., 9, 417-432.
- Melvin, G.L., 1968: The development of thunderstorm complexes and their associated vertical transports. S.M. Thesis, Dept. of Met., MIT, Cambridge, Mass., 65 pp.
- Nason, C.K., 1965: Mesoscale precipitation patterns in central New England. S.M. Thesis, Dept. of Met., MIT, Cambridge, Mass., 99 pp.

- Newell, R.E., 1960: A study of tropospheric cellular convection and its role in vertical transport from weather radar and radio-activity data. Sc.D. Thesis, Dept. of Met., MIT, Cambridge, Mass., 151 pp.
- Sanders, F., and D.A. Olson, 1967: The release of latent heat of condensation in a simple precipitation forecast model. J. Appl. Met., 6, 229-236.
- Shuman, F.G. and J.B. Hovermale, 1968: An operational six-layer primitive equation model. J. Appl. Met., 7, 525-547.
- Tracton, M.S., 1968: The role of cellular convection within an extra-tropical cyclone. S.M. Thesis, Dept. of Met., MIT, Cambridge, Mass., 51 pp.
- U.S. Dept. of Commerce, Weather Bureau, 1970: Numerical Weather Prediction Activities. National Meteorological Center, Silver Spring, Md. 51 pp.
- Younkin, R.J., J.A. LaRue and F. Sanders, 1965: The objective prediction of clouds and precipitation using vertically integrated moisture and adiabatic vertical motions. S. Appl. Met., 4, 3-17.